PCCP

COMMUNICATION

Cite this: *Phys. Chem. Chem. Phys.*, 2018, **20**, 16913

Received 11th May 2018,
Accepted 5th June 2018

DOI: 10.1039/c8cp03019g

rsc.li/pccp

Vibrational quantum graphs and their application to the quantum dynamics of CH_5^+

Csaba Fábri *[ab] and Attila G. Császár [ab]

The first application of quantum graphs to the vibrational quantum dynamics of molecules is reported. The quantum-graph model is applied to the quasistructural molecular ion CH_5^+, whose nuclear dynamics challenges the traditional understanding of chemical structures and molecular spectra. The vertices of the quantum graph represent versions of the equilibrium structure with distinct atom numbering, while the edges refer to collective nuclear motions transforming the versions of the equilibrium structure into one another. These definitions allow the mapping of the complex vibrational quantum dynamics of CH_5^+ onto the motion of a particle confined in a quantum graph. The quantum-graph model provides a simple understanding of the low-energy vibrational quantum dynamics of CH_5^+ and is able to reproduce the low-lying vibrational energy levels of CH_5^+ (and CD_5^+) with remarkable accuracy.

The introduction of the tools of mathematical analysis (algebraic and differential equations, orthogonal functions, *etc.*) into natural sciences in the 17th century revolutionized them and resulted in a long and steady progress. Graph theory,[1] a branch of mathematics whose name originates from chemistry,[2] entered late into these sciences but has proved to be important for the study of complex phenomena not only in physics and chemistry but also in other disciplines, including computer science, social sciences and biology.[3] Conventional applications of graphs and networks in chemistry concern problems related to chemical graphs,[4] spectroscopic networks,[5] thermochemical networks,[6] and cheminformatics and computer-aided drug design.[7] Models based on quantum graphs have been used in chemistry[8–11] as well as in physics.[12–17] Surveys investigating the mathematical properties of quantum graphs have also been published.[18,19] Hereby, we introduce quantum graphs to describe vibrations of certain molecular systems, where traditional treatments fail to provide a good zeroth-order picture.

[a] *Laboratory of Molecular Structure and Dynamics, Institute of Chemistry, Eötvös Loránd University, Pázmány Péter sétány 1/A, H-1117 Budapest, Hungary*
[b] *MTA-ELTE Complex Chemical Systems Research Group, P.O. Box 32, H-1518 Budapest 112, Hungary. E-mail: ficsaba@caesar.elte.hu*

The traditional understanding and interpretation of molecular structures and spectra rely on the Born–Oppenheimer approximation and involve simple zeroth-order models such as the rigid rotor and the harmonic oscillator.[20] An important feature of this traditional approach is the approximate separation of electronic, vibrational and rotational degrees of freedom, the latter two describing the motion of the nuclei. Well-established extensions based on perturbation theory are able to systematically improve the results provided by the zeroth-order models and have been applied with remarkable accuracy even if the molecule under investigation exhibits large amplitude motions (*e.g.*, internal rotation of a methyl (CH_3) group or the umbrella motion in ammonia (NH_3)).[20,21] However, in the case of quasistructural molecules,[22] there are multiple accessible minima on the potential energy surface (PES), the separation of the different internal degrees of freedom breaks down spectacularly, and the conventional nearly-rigid "ball and stick" image of the molecular structure must be abandoned. Attempts to interpret molecular spectra of quasistructural molecules in terms of the conventional harmonic oscillator and rigid rotor models fail miserably. A striking example from the family of quasistructural molecules is protonated methane (CH_5^+, also called methonium), the prototype of penta-(or higher-)coordinated "non-classical" carbocations showing rich and exotic chemistry.[23] Besides its chemical relevance, CH_5^+, owing to its unique rotation–vibration quantum dynamics and highly complex and congested infrared spectra even at very low temperatures (few K), has puzzled the community of high-resolution molecular spectroscopists for decades.[24–28] CH_5^+ provides a challenging playground for the development of novel theoretical methods[29–33] that are able to solve the rotation–vibration Schrödinger equation for polyatomic molecules in a numerically exact way in the fourth age of quantum chemistry.[34] Electronic structure studies revealed that the equilibrium structure (the minimum on the PES) of CH_5^+ can be characterized as a strongly bound CH_3^+ unit attached to a H_2 moiety, with a three-center two-electron bond between the two units (see the structures in Fig. 1).[35] It was even concluded that the barrier to the complete scrambling of the five protons is essentially zero, implying that CH_5^+ is a "highly fluxional

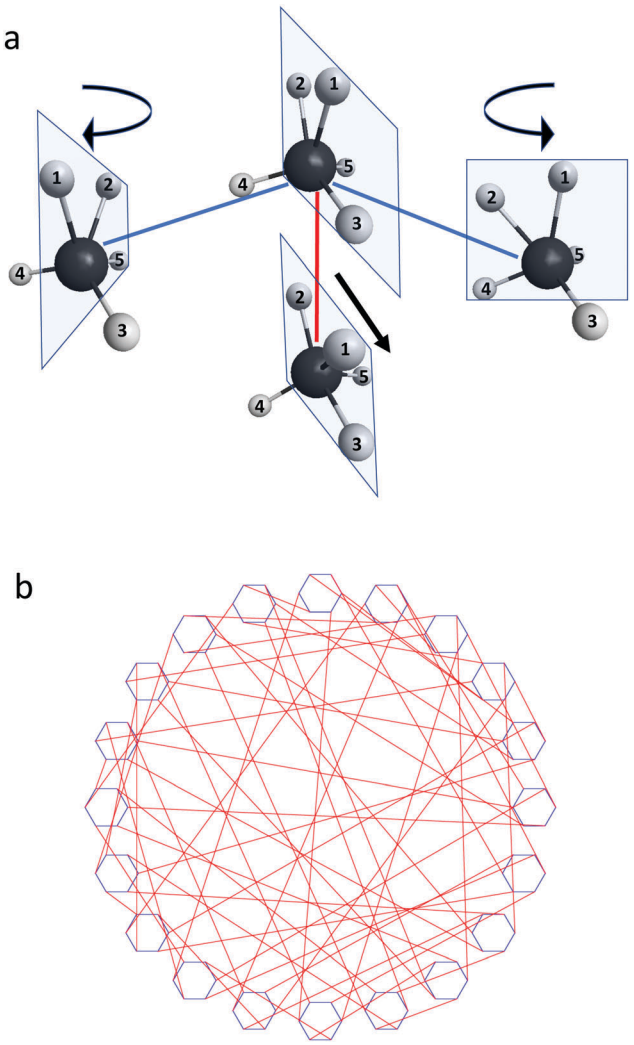

Fig. 1 (a) Four selected symmetry-equivalent versions of the equilibrium structure of CH_5^+. The C_s point-group symmetry of the equilibrium structure is indicated by the symmetry planes drawn. The uppermost version is connected to three other versions by the internal rotation (blue) and flip (red) motions. (b) Pictorial representation of the quantum graph applied to the quantum-dynamical description of the low-energy vibrations of CH_5^+. The 120 internal rotation and 60 flip edges connecting the 120 equivalent vertices (versions) are indicated by blue and red lines, respectively.

molecule without a definite structure".[35] Other studies found that in CH_5^+, in contrast to the vast majority of molecules, it is virtually impossible to separate the vibrational and rotational degrees of freedom.[31,36] In view of these peculiarities it is not surprising that the quantum states of CH_5^+ have escaped an analytical description in terms of simple zeroth-order models. One promising approach to remedy the lack of appropriate zeroth-order models is the recently developed five-dimensional rigid rotor model.[37–39] In this communication we develop an alternative zeroth-order model, the simple and intuitive quantum-graph model, and demonstrate that it is able to decipher the intricate details of the vibrational quantum dynamics of CH_5^+ in a natural way. To the best of our knowledge, this is the first application of the quantum-graph model to the vibrational quantum dynamics of molecules.

A graph is a collection of v vertices that are connected by e edges representing linkages between vertices. In order to construct the one-dimensional Schrödinger equation for a particle confined into a quantum graph, it is necessary to postulate that each edge possesses a length (metric graph). In what follows we provide only a concise summary of quantum-graph theory relevant for this study and refer to the literature[18,19] for details. The Hamiltonian expressed in atomic units has the simple form

$$\hat{H} = -\frac{1}{2}\frac{\mathrm{d}^2}{\mathrm{d}x^2} + V(x), \tag{1}$$

where $x \in [0,L_j]$ is a mass-scaled local coordinate defined along the jth edge of length L_j ($j = 1,\ldots,e$). Although it is possible to assign one-dimensional potentials to the edges, we limit our discussion to the case of free motion ($V(x) = 0$), though our aim is to treat vibrational motions. The eigenfunctions of $\hat{H}$ along the jth edge of the graph are superpositions of outgoing and incoming one-dimensional plane waves,

$$\psi_j(x) = a_j \exp(ikx) + b_j \exp(-ikx), \tag{2}$$

with the corresponding energy eigenvalues $E_k = k^2/2$. The energy levels are quantized by using the familiar von Neumann boundary conditions[18,19]

$$\begin{aligned} \psi_1(0) &= \psi_2(0) = \cdots = \psi_{d_l}(0) \\ \sum_{\alpha=1}^{d_l} \frac{\mathrm{d}\psi_\alpha}{\mathrm{d}x}\bigg|_{x=0} &= 0, \end{aligned} \tag{3}$$

where α enumerates those edges that are connected to the lth vertex of degree d_l ($l = 1,\ldots,v$). The two boundary conditions of eqn (3) express the continuity of the wave function and the conservation of the quantum flux, respectively (see ref. 10 for a mathematically rigorous description). The implementation of the boundary conditions of eqn (3) can be elegantly reformulated as an eigenvalue problem of a unitary matrix $\mathbf{S}(k)$, also called the scattering matrix, whose elements parametrically depend on k and are determined by the connectivity of the quantum graph and the edge lengths.[18,19] The quantization conditions are obtained in the form

$$\det(\mathbf{S}(k) - \mathbf{I}) = 0, \tag{4}$$

where $\mathbf{I}$ is the identity matrix whose dimension equals the dimension of $\mathbf{S}(k)$.[18,19]

In order to apply graph theory to practical problems, it is necessary to specify the meaning of the vertices and edges. If the quantum-graph model is employed to describe the vibrational quantum dynamics of molecules, it seems obvious to identify the vertices as distinct versions[21] of the equilibrium structure, while the edges represent collective motions of the nuclei converting different versions into each other. In the case of CH_5^+, the 5! = 120 symmetry-equivalent versions of the equilibrium structure can be generated by the 120 possible permutations of the five protons.[21] A selected version of C_s point-group symmetry is depicted in the upper panel of Fig. 1, where protons 1 and 2 belong to the H_2 unit sitting on top of a CH_3^+ tripod formed by protons 3, 4, and 5. The two motions

interconverting the 120 equivalent versions correspond to the clockwise and counterclockwise internal rotations of the H_2 unit by $\pi/3$ (represented by the two blue lines in the upper panel of Fig. 1), and to the flip motion that exchanges a pair of protons (2 and 3 in the upper panel of Fig. 1, where the flip motion is shown by the red line) between the H_2 and CH_3^+ units.[40] The barriers hindering the internal rotation and flip motions are only about 30 cm^{-1} and 300 cm^{-1}, respectively, allowing facile exchange of the protons. This implies that the molecular symmetry group[21] of CH_5^+ is $S_5^* = S_5 \otimes \{E,E^*\}$, where S_5 denotes the symmetric group of degree five whose elements permute the five equivalent protons, while E and E^* refer to the identity and space inversion operations. As other stationary points on the PES of CH_5^+ have appreciably higher energies than the internal rotation and flip barriers,[35] it is plausible that motions other than the internal rotation and flip motions can be disregarded as long as one is interested in the low-energy vibrational quantum dynamics of CH_5^+. The lower panel of Fig. 1 shows the structure of the quantum graph of CH_5^+. In total, there are 120 equivalent vertices of degree three connected by 120 internal rotation (in blue) and 60 flip (in red) edges forming the CH_5^+ quantum graph. Each of the 20 blue hexagons in Fig. 1 represents six versions that are related by internal rotations of the H_2 unit. Each hexagon is connected to six other hexagons by six flip edges. As all vertices are equivalent and there are only two different edge types, the quantum graph of CH_5^+ can be parameterized with two different edge lengths, L_1 for the internal rotation edges and L_2 for the flip edges.

In order to perform numerical computations with the quantum-graph model, we need to obtain numerical values for L_1 and L_2. A simple and approximate method to derive L_1 and L_2 is based on the two-dimensional (2D) rotor Hamiltonian

$$\hat{H}_{\mathrm{rotor}} = -\frac{1}{2\theta}\frac{\mathrm{d}^2}{\mathrm{d}\varphi^2} = -\frac{1}{2}\frac{\mathrm{d}^2}{\mathrm{d}x^2}, \qquad (5)$$

where $\varphi \in [0,\varphi_{\max}]$, θ is the moment of inertia and the local coordinate is defined as $x = \sqrt{\theta}\varphi$, resulting in $L = \sqrt{\theta}\varphi_{\max}$ for the edge-length parameter. Both the internal rotation and flip motions can be described within the framework of the 2D rotor model by treating the $H_2(D_2)$ unit or the H(D) atom involved in the flip motion as a 2D rotor and freezing the motion of the other nuclei. We have used $\theta = mr_1^2/2$ and $\theta = mr_2^2$ for the internal rotation and flip motions, respectively, where m is the mass of H(D), r_1 is the bond length in the $H_2(D_2)$ unit and r_2 is the distance between the carbon and the H(D) atom involved in the flip process, while the $\varphi_{\max}$ values associated with the internal rotation and flip motions are estimated to be $\pi/3$ and $3\pi/20$, respectively. These assumptions yield the approximate formulae $L_1 = \pi/(3\sqrt{2})\sqrt{m}r_1$ and $L_2 = 3\pi/20\sqrt{m}r_2$, and the *ab initio* edge-length values of $L_1 = 58.5\sqrt{m_e}a_0$ and $L_2 = 45.1\sqrt{m_e}a_0$ for CH_5^+ and $L_1 = 82.7\sqrt{m_e}a_0$ and $L_2 = 63.7\sqrt{m_e}a_0$ for CD_5^+ (employing r_1 and r_2 values estimated from the equilibrium structure), where m_e and a_0 stand for the electron mass and the Bohr radius, respectively. Tables 1 and 2 compare the quantum-graph vibrational energy levels computed with the *ab initio* L_1 and L_2 parameters (*ab initio* column) to their numerically exact quantum-chemical counterparts (12D(ref) and 7D(ref) columns) taken from ref. 30, 32 and 33. The 12D(ref) and 7D(ref) results, computed using variational nuclear motion codes,[30,32,33] serve as accurate reference data. For CH_5^+ both the 12D ("basis IV min" results taken from ref. 30, treating all vibrational degrees of freedom) and 7D bend (considering only the seven bend vibrational degrees of freedom and freezing the five stretch modes[30,32,33]) variational vibrational energy levels are available, while for CD_5^+ there are only 7D bend variational vibrational energy levels (computed with the GENIUSH program package[33,34,41,42] as part of this study). Although the *ab initio* quantum-graph energy levels show substantial deviations from the corresponding variational reference vibrational energy levels (they underestimate the reference values for all eigenstates shown in Tables 1 and 2), we can conclude that the vibrational energy level patterns are qualitatively reproduced using the quantum-graph model for both CH_5^+ and CD_5^+.

In order to improve the accuracy of the quantum-graph vibrational energy levels, one can define an objective function

Table 1 Low-lying vibrational energy levels (in cm^{-1}) of CH_5^+ with S_5^* symmetry labels (Γ). The 7D bend and 12D variational vibrational energy levels[30,32,33] (7D(ref) and 12D(ref), respectively) are compared to their counterparts obtained using the quantum-graph model (7D(fit), 12D(fit) and *ab initio*)

Γ	7D(ref)	7D(fit)	12D(ref)	12D(fit)	*ab initio*
A_1^+	0.0	0.0	0.0	0.0	0.0
G_2^-	9.8	11.4	10.4	10.3	6.2
H_1^+	20.3	22.2	21.7	20.5	14.9
H_2^-	41.1	39.6	39.8	36.4	27.8
G_1^+	49.3	44.8	39.3	38.7	16.4
I^-	58.2	49.7	47.3	44.1	22.8
H_2^+	59.1	50.2	52.3	45.9	33.0
I^+	111.4	95.2	89.4	84.6	49.7
G_2^-	112.3	100.9	85.6	87.4	45.5
H_1^-	113.4	96.0	96.2	87.5	56.5
H_1^+	121.3	112.4	106.5	102.8	58.5
H_2^-	139.1	148.7	137.1	137.4	100.5
G_1^+	154.2	182.0	153.0	165.1	111.0
A_2^-	197.8	284.5	n/a	258.3	147.7

Table 2 Low-lying vibrational energy levels (in cm^{-1}) of CD_5^+ with S_5^* symmetry labels (Γ). The 7D bend variational vibrational energy levels (7D(ref)) are compared to their counterparts obtained using the quantum-graph model (7D(fit) and *ab initio*)

Γ	7D(ref)	7D(fit)	*ab initio*
A_1^+	0.0	0.0	0.0
G_2^-	4.1	4.6	3.1
H_1^+	10.0	8.9	7.4
H_2^-	17.4	15.9	13.9
G_1^+	18.7	18.1	8.2
I^-	21.8	20.1	11.4
H_2^+	23.0	20.2	16.5
I^+	40.5	38.4	24.9
G_2^-	40.8	40.8	22.8
H_1^-	41.6	38.6	28.3
H_1^+	47.4	45.2	29.3
H_2^-	59.4	59.8	50.3
G_1^+	67.7	73.3	55.6
A_2^-	84.2	114.5	73.9

as the root-mean-square deviation between the quantum-graph and variational reference vibrational energy levels and minimize this objective function in the parameter space of L_1 and L_2, yielding refined values for the edge lengths L_1 and L_2. For CH_5^+, the fit gives the values of $L_1 = 62.5\sqrt{m_e}a_0$ and of $L_2 = 4.5\sqrt{m_e}a_0$ for the 12D reference data, $L_1 = 61.2\sqrt{m_e}a_0$ and $L_2 = 1.0\sqrt{m_e}a_0$ for the 7D reference data. For CD_5^+, $L_1 = 96.7\sqrt{m_e}a_0$ and $L_2 = 1.1\sqrt{m_e}a_0$ for the 7D reference data. Tables 1 and 2 compare the fitted quantum-graph vibrational energy levels (12D(fit) and 7D(fit) columns) to the variational reference vibrational energy levels (12D(ref) and 7D(ref) columns). The results presented in Tables 1 and 2 clearly show that fitting greatly improves the accuracy of the quantum-graph vibrational energy levels. The simple quantum-graph model with zero potential is able to reproduce the variational vibrational energy levels of CH_5^+ and CD_5^+ surprisingly well, except for the highest energy level (of A_2^- symmetry) which was therefore excluded from the fit.

Regarding the higher-lying vibrational energy levels, we have found that the agreement between the variational and the quantum-graph vibrational energy levels deteriorates and it seems that certain vibrational energy levels are missing from the set of quantum-graph vibrational energy levels. This finding is not surprising as the quantum-graph model considers only the internal rotation and flip motions and thus cannot be expected to account for the additional degrees of freedom. We believe that the internal rotation and flip motions are necessary and at the same time sufficient for understanding the low-energy vibrational quantum dynamics of CH_5^+, and without the inclusion of these two motions no quantum-dynamical model is able to provide sensible results for the quantum dynamics of CH_5^+.

At first glance it may be surprising that a crude quantum-graph model with zero potential is able to reproduce the lowest vibrational energy levels of the six-atomic CH_5^+ and CD_5^+ molecular ions. The use of the term ''crude'' is justified by at least four different features of the quantum-graph model: (a) a single-particle problem is considered in one dimension, (b) the motion of the particle is not hindered by the potential, (c) only the internal rotation and flip motions are included in the model, and (d) the effective masses associated with the two motions are assumed to be constant. We believe that the strength of the quantum-graph model is that even though the particle is assumed to move freely along the edges of the quantum graph, some of the features of the PES of CH_5^+ are implicitly taken into account as the connectivity of the quantum graph is determined by certain characteristics of the PES. This observation is related to our qualitative conclusions drawn in ref. 33 and summarized as follows: (a) as the barriers separating minima on the PES of CH_5^+ are low, a model based on tunneling between the 120 equivalent potential wells, leading to what is called a tunneling matrix, fails to explain the peculiar vibrational energy level pattern of CH_5^+ and (b) in spite of the low barriers the motion of the five protons is not completely free, any pair of protons approaching each other causes large potential energy values; therefore, the motion of the protons is strongly correlated and CH_5^+ cannot be thought of as a system made up by five uncoupled rotors. In view of these statements, we conjecture that the quantum dynamics of CH_5^+ is best described by a model based on the concept of quasi-free motion. It should be obvious at this stage that the general and simple quantum-graph model is able to capture the basic features of the quasi-free motion in a natural way by restricting the system to move along appropriately chosen edges. In the case of CH_5^+, the system is allowed to sample all 120 potential energy minima by moving freely along the edges representing the internal rotation and flip motions.

At this point, it is worth stressing the analogy between the quantum-graph model and the elementary particle-in-a-box model. The application of the quantum-graph model is equivalent to mapping the multidimensional vibrational quantum dynamics on the much simpler problem of a particle confined in an appropriately designed quantum graph.

Although it may seem that the quantum-graph model is restricted to highly symmetric molecular systems, the treatment of less symmetric systems is expected to pose no difficulty. One obvious process leading to lower symmetries corresponds to the partial deuteration of CH_5^+. Our preliminary analysis suggests that even though partial deuteration does not change the connectivity of the quantum graph shown in Fig. 1, more than two edge lengths are needed to parameterize the quantum graph as neither the vertices nor the edges associated with the same motion remain fully equivalent. We are convinced that the quantum-dynamical theory of quasistructural (at least extremely flexible) molecules and complexes will benefit from the simple and general idea presented in this communication.

Conflicts of interest

There are no conflicts of interest to declare.

Acknowledgements

C. F. and A. G. C. are grateful to NKFIH for grants No. PD124699 and K119658, respectively. Our research also received support from the grant VEKOP-2.3.2-16-2017-00014, supported by the European Union and the State of Hungary and co-financed by the European Regional Development Fund. The authors thank Viktor Szalay, Tucker Carrington, Tamás Szidarovszky and Roland Tóbiás for fruitful discussions.

References

1 L. Euler, *Comment. Acad. Sci. U. Petrop.*, 1736, **8**, 128–140.
2 J. J. Sylvester, *Nature*, 1878, **17**, 284.
3 M. E. J. Newman, *Networks: An Introduction*, Oxford University Press, Oxford, 2010.
4 N. Trinajstić, *Chemical Graph Theory*, CRC-Press, Boca Raton, FL, 1992.
5 A. G. Császár and T. Furtenbacher, *J. Mol. Spectrosc.*, 2011, **266**, 99–103.

6 B. Ruscic, R. E. Pinzon, M. L. Morton, G. von Laszevski, S. J. Bittner, S. G. Nijsure, K. A. Amin, M. Minkoff and A. F. Wagner, *J. Phys. Chem. A*, 2004, **108**, 9979–9997.
7 A. Leach and V. Gillet, *An Introduction to Chemoinformatics*, Springer, 2007.
8 L. Pauling, *J. Chem. Phys.*, 1936, **4**, 673–677.
9 H. Kuhn, *Helv. Chim. Acta*, 1949, **32**, 2247–2272.
10 K. Ruedenberg and C. W. Scherr, *J. Chem. Phys.*, 1953, **21**, 1565–1581.
11 C. W. Scherr, *J. Chem. Phys.*, 1953, **21**, 1582–1596.
12 M. Richardson and N. Balazs, *Ann. Phys.*, 1972, **73**, 308–325.
13 T. Kottos and U. Smilansky, *Phys. Rev. Lett.*, 1997, **79**, 4794–4797.
14 T. Kottos and U. Smilansky, *Phys. Rev. Lett.*, 2000, **85**, 968–971.
15 H. Schanz and U. Smilansky, *Phys. Rev. Lett.*, 2000, **84**, 1427–1430.
16 G. Montambaux, *Phys.-Usp.*, 2001, **44**, 65–68.
17 S. Gnutzmann and U. Smilansky, *Adv. Phys.*, 2006, **55**, 527–625.
18 P. Kuchment, *Wave Random Media*, 2002, **12**, R1–R24.
19 G. Berkolaiko and P. Kuchment, *Introduction to Quantum Graphs*, American Mathematical Society, 2013, vol. 186.
20 *Handbook of High-Resolution Spectroscopy*, ed. M. Quack and F. Merkt, Wiley, Chichester, 2011.
21 P. Bunker and P. Jensen, *Molecular Symmetry and Spectroscopy*, NRC Research Press, 2006.
22 C. Fábri, J. Sarka and A. G. Császár, *J. Chem. Phys.*, 2014, **140**, 051101.
23 G. A. Olah, *My Search for Carbocations and Their Role in Chemistry*, 1994, pp. 149–176.
24 E. T. White, J. Tang and T. Oka, *Science*, 1999, **284**, 135–137.
25 O. Asvany, P. Padma Kumar, B. Redlich, I. Hegemann, S. Schlemmer and D. Marx, *Science*, 2005, **309**, 1219–1222.
26 S. D. Ivanov, O. Asvany, A. Witt, E. Hugo, G. Mathias, B. Redlich, D. Marx and S. Schlemmer, *Nat. Chem.*, 2010, **2**, 298–302.
27 O. Asvany, K. M. T. Yamada, S. Brünken, A. Potapov and S. Schlemmer, *Science*, 2015, **347**, 1346–1349.
28 S. Brackertz, S. Schlemmer and O. Asvany, *J. Mol. Spectrosc.*, 2017, **342**, 73–82.
29 X. Huang, A. B. McCoy, J. M. Bowman, L. M. Johnson, C. Savage, F. Dong and D. J. Nesbitt, *Science*, 2006, **311**, 60–63.
30 X.-G. Wang and T. Carrington, *J. Chem. Phys.*, 2008, **129**, 234102.
31 R. Wodraszka and U. Manthe, *J. Phys. Chem. Lett.*, 2015, **6**, 4229–4232.
32 X.-G. Wang and T. Carrington, *J. Chem. Phys.*, 2016, **144**, 204304.
33 C. Fábri, M. Quack and A. G. Császár, *J. Chem. Phys.*, 2017, **147**, 134101.
34 A. G. Császár, C. Fábri, T. Szidarovszky, E. Mátyus, T. Furtenbacher and G. Czakó, *Phys. Chem. Chem. Phys.*, 2012, **14**, 1085–1106.
35 P. R. Schreiner, S.-J. Kim, H. F. Schaefer III and P. von Ragué Schleyer, *J. Chem. Phys.*, 1993, **99**, 3716–3720.
36 H. Schmiedt, S. Schlemmer and P. Jensen, *J. Chem. Phys.*, 2015, **143**, 154302.
37 H. Schmiedt, P. Jensen and S. Schlemmer, *Phys. Rev. Lett.*, 2016, **117**, 223002.
38 H. Schmiedt, P. Jensen and S. Schlemmer, *Chem. Phys. Lett.*, 2017, **672**, 34–46.
39 H. Schmiedt, P. Jensen and S. Schlemmer, *J. Mol. Spectrosc.*, 2017, **342**, 132–137.
40 M. Kolbuszewski and P. R. Bunker, *J. Chem. Phys.*, 1996, **105**, 3649–3653.
41 E. Mátyus, G. Czakó and A. G. Császár, *J. Chem. Phys.*, 2009, **130**, 134112.
42 C. Fábri, E. Mátyus and A. G. Császár, *J. Chem. Phys.*, 2011, **134**, 074105.